the gate coordinate is fast compared to motion along x. This has been demonstrated above by the correspondence between case a and the one-dimensional analysis. Even so, a meaningful discussion of the gating mechanism would not be possible within the context of the simple one-dimensional reaction profile. We should also point out that, based on results of previous computational studies of the free-energy cost of tyrosine ring rotations in proteins,[10] it may not always be straightforward to obtain adequate equilibrium sampling of the free-energy barrier of a gated reaction along the primitive reaction coordinate. A "best" reaction coordinate which is a combination of the primitive and gate coordinates will facilitate sampling procedures.

A number of important reactive processes in condensed phases may not only be gated, but have rates which are limited or at least influenced by the gate-opening step itself. For these reactions (which correspond to case b in our analysis), the conventional picture is clearly inadequate in making successful predictions of the rate or in understanding the mechanism. For such reactions the inclusion of auxiliary coordinates is essential. Analysis based on a multidimensional reaction profile has the advantage of encompassing all of the various limiting regimes and displaying the interplay of a variety of factors within a single theoretical framework. For example, the extent to which a reaction is gated or gate-limited may vary with changes in environmental parameters that affect gate motion differently than primitive coordinate motion.

Clearly, the specific example of gating presented here lacks the necessary generality to encompass the diversity of gated reactions. For example, in our simple picture there are free-energy minima for gate-open states. These minima (A′ and B′) may not exist in every case. However, the model does serve to illustrate the central ideas pertaining to the concept of gated reactions in a fairly general way and can readily be extended to other specific situations. It seems apparent that the inclusion of auxiliary coordinates into reaction profile maps will be an essential tool for studying complex reactions that occur in condensed phases.

Acknowledgment. This work was supported in part by grants from the Petroleum Research Fund, administered by the American Chemical Society, the Research Corporation (Tennessee Tech), the Robert A. Welch Foundation, and NSF (Houston). J.A.M. is an Alfred P. Sloan Fellow and the recipient of NIH Research Career Development and Camille and Henry Dreyfus Teacher-Scholar Awards.

Experimental and Computed Chiroptical Properties of Thioketones[1]

David A. Lightner,*[2a] Thomas D. Bouman,*[2b] W. M. Donald Wijekoon,[2a] and Aage E. Hansen[2c]

Contribution from the Departments of Chemistry, University of Nevada, Reno, Nevada 89557, and Southern Illinois University, Edwardsville, Illinois 62026, and the Department of Physical Chemistry, H. C. Ørsted Institute, DK-2100 Copenhagen Ø, Denmark. *Received May 17, 1983*

Abstract: (+)-(1*S*,3*R*)-4*S*(a)-Methyladamantane-2-thione (**1**), (+)-(1*S*,3*R*)-4*R*(e)-methyladamantane-2-thione (**3**), and (+)-(1*S*,3*R*)-4,4-dideuterioadamantane-2-thione (**5**) were prepared and their circular dichroism (CD) spectra measured and compared with those of the corresponding ketones. The long-wavelength n–π^* CD transitions of the thiones and parent ketones agree in sign and magnitude. Ab initio calculations on thioacetone and methyl ethyl thioketone in the random-phase approximation (RPA) in several basis sets lead to assignment of the two lowest energy observed bands as n–π^* and π–π^* and a third band composed of closely spaced and n–4s and σ–π^* excitations. Similar calculations on **1** and **3** and their keto analogues yield n–π^* rotatory strengths (R) in excellent agreement with experiment and support the applicability of the ketone octant rule to thioketones. An origin-independent analysis of the computed R values suggests that the same mechanism for n–π^* optical activity operates in both classes of compounds.

In contrast to ketones, there are comparatively few known saturated alkyl thioketones.[3] This is in part due to the greater reactivity of C=S (vs. C=O), particularly the greater tendencies toward dimerization and trimerization as well as tautomerization of C=S to the thioenol.[3-5] Consequently most known, stable thioketones are either incapable of enolizing, e.g., thiofenchone,[6] or enolize only with considerable difficulty, e.g., thiocamphor and adamantanethione.[3] These orange-red, saturated alkyl thioketones exhibit an interesting, weak low-lying electronic transition near 500 nm that is generally thought to be similar in nature to the ketone n–π^* transition.[3-8] Theoretical calculations on the electronic spectrum of thioformaldehyde[9a,b] (where the band occurs at 610 nm)[10] and thioacetone[9c] unanimously support this assignment. Solution spectra of thioketones show, in addition, two

(1) The Octant Rule. 11; for part 10 see: Rodgers, S. L.; Kalyanam, N.; Lightner, D. A. *J. Chem. Soc., Chem. Commun.* **1982**, 1040–1042.
(2) (a) University of Nevada, Reno. (b) Southern Illinois University, Edwardsville. (c) H. C. Ørsted Institute.
(3) For leading references, see: Greidenaus, J. W. *Can. J. Chem.* **1970**, *48*, 3530–3536.
(4) (a) Mayer, R.; Morgenstern, J.; Fabian, J. *Angew. Chem., Int. Ed. Engl.* **1964**, *3*, 277–286. (b) Fabian, J.; Mayer, R. *Spectrochim. Acta* **1964**, *20*, 299–304.
(5) Campaigne, E. In "The Chemistry of the Carbonyl Group"; Patai, S., Ed.; Interscience: New York, 1966; Chapter 17.
(6) Wijekoon, W. M. D.; Bunnenberg, E.; Records, R.; Lightner, D. A. *J. Phys. Chem.* **1983**, *87*, 3034–3037.
(7) Ballard, R. E.; Mason, S. F. *J. Chem. Soc.* **1963**, 1624–1628.
(8) (a) McMurry, H. L. *J. Chem. Phys.* **1941**, *9*, 231–240, 241–251. (b) Sidman, J. W. *Chem. Rev.* **1958**, *58*, 689–713. (c) Rosengren, K. J. *Acta Chem. Scand.* **1962**, *16*, 2284–2292.
(9) (a) Bruna, P. J.; Peyerimhoff, S. D.; Buenker, R. J.; Rosmus, P. *Chem. Phys.* **1974**, *3*, 35–53. (b) Burton, P. G.; Peyerimhoff, S. D.; Buenker, R. J. *Ibid.* **1982**, *73*, 83–98. (c) Bruna, P. J.; Buenker, R. J.; Peyerimhoff, S. D. *Ibid.* **1977**, *22*, 375–382.
(10) (a) Judge, R. H.; Moule, D. C.; King, G. W. *J. Mol. Spectrosc.* **1980**, *81*, 37–59. (b) Judge, R. H.; Drury-Lessard, C. R.; Moule, D. C. *Chem. Phys. Lett.* **1978**, *53*, 82–83.

0002-7863/84/1506-0934$01.50/0

partially resolved, intense bands in the UV at 235 and 213 nm; the solvent dependence of the band maxima supports their assignment as a $\pi-\pi^*$ excitation and an $n-\sigma^*$ excitation, respectively.[4b] These latter assignments are by no means certain, however.[7,8,10] Absorption and magnetic circular dichroism (MCD) studies have been reported recently for the $n-\pi^*$ transition of adamantanethione, bicyclo[2.2.1]heptane-2-thione, and 2,4-dimethylpentane-3-thione.[11] A very weak band appearing at ca. 565 nm was assigned as the $^3n-\pi^*$ excitation on the basis of what appears to be an *A* term in the MCD spectrum.[11] A similar excitation has been observed at 689 nm and analyzed in thioformaldehyde as well.[10a] Rydberg-type excitations have been observed in $H_2C{=}S$ in the vacuum UV at 212, 188, and 181 nm, along with a broad band (presumably $\pi-\pi^*$) centered around 200 nm.[10b] Rydberg series have also been studied in the spectra of tetramethyl-1,3-cyclobutanedithione and the corresponding thiocyclobutanone.[12]

As of this writing, very few optically active thioketones have been prepared, and even fewer have been examined by optical rotatory dispersion (ORD) or circular dichroism (CD). Thus, in 1961, Djerassi and Herbst[13] published the first ORD spectra of two 17-thioketo steroids (androstane-17-thione and 3β-hydroxy-Δ^5-androstene-17-thione) and 3-oxo-Δ^4-pregnene-20-thione. The (+) Cotton effect (CE) signs observed[13] for the long-wavelength transitions of the 17-thiones correlate well with the (+) $n-\pi^*$ CEs of the corresponding ketones.[14] On the basis of the data, however, it was unclear at the time whether the octant rule[14,15] could be applied generally to thioketones. Shortly thereafter, Ballard and Mason[7] compared the long-wavelength CD and UV transitions of the 7-keto steroid epiandrosterone (ϵ_{288}^{max} 40, $\Delta\epsilon_{290}^{max}$ +3.0) and its thione (ϵ_{482}^{max} 13, $\Delta\epsilon_{500}^{max}$ +1.3), and supported the idea that the long-wavelength thioketone transition is of the $n-\pi^*$ type. Emeis and Oosterhoff[16] studied the $n-\pi^*$ CD and circularly polarized luminescence (CPL) of *trans*-β-hydrindanone [(1*S*,6*S*-bicyclo[4.3.0]nonan-8-one: ϵ_{299}^{max} 29, $\Delta\epsilon_{310}^{max}$ +6.0] and its thio analogue (ϵ_{510}^{max} 18, $\Delta\epsilon_{542}^{max}$ +4.5) and analyzed the vibrational structure. The absence of CPL in the longest wavelength part of the spectrum supported the triplet–singlet nature of that transition. No other CD spectra of saturated alkyl thioketones appeared until the long-wavelength CD transition ($\Delta\epsilon_{507}^{max}$ −0.38) of (1*S*)-4,4-dideuterioadamantane-2-thione was published by Numan, Neuwese, and Wynberg.[17a] In agreement with the parent ketone ($\Delta\epsilon_{293}^{max}$ −0.089)[17b] the CE sign was found to be negative. Very recently, Schippers and Dekkers[18] have measured the CD and CPL of the $n-\pi^*$ band of the same dideuterio thioketone and have studied the barrier to inversion in the excited state. Finally, we have lately measured the CD of thiofenchone in conjunction with a study of its seleno analogue.[6]

The purpose of this paper is twofold. First, we examine the applicability of the ketone octant rule[15,19] to thioketones based upon the adamantanethione skeleton. Because the 3-equatorial position of cyclohexanone has been a well-studied,[19-21] confirmed safe position for consignate[21] alkyl groups, we prepared and examined the sterochemically well-defined (1*S*,3*R*)-4*R*(e)-methyladamantane-2-thione (**3**), where the lone dissymmetric perturber is a methyl group. We also prepared and examined the axial epimer, (1*S*,3*R*)-4*S*(a)-methyladamantane-2-thione (**1**), because the parent axial-methyl ketone has been shown to be one clear example,[22,23] of relatively few known, where the methyl group can make a dissignate octant contribution.[1,22-24] Finally, the surprisingly large magnitude ($\Delta\epsilon_{507}^{max}$ −0.38)[25] reported for the long-wavelength CE of (1*S*,3*R*)-4,4-dideuterioadamantane-2-thione (**5**)[17a] prompted us to prepare and examine the same compound ourselves, particularly in view of the much lower value ($\Delta\epsilon_{293}^{max}$ −0.089) exhibited by the parent ketone.[17b]

Chart I

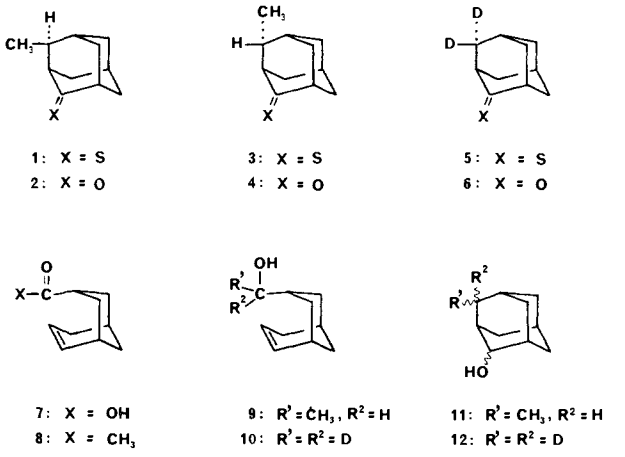

The second purpose is to characterize the electronic states of thioketones in the range 190–600 nm and to make comparisons with ketone spectra. Our study encompasses UV/CD measurements of compounds **1–6** (Chart I), as well as ab initio quantum-mechanical calculations on **1–4** and on the smaller model systems thioacetone and methyl ethyl thioketone. Although Peyerimhoff and co-workers have carried out extensive calculations on the spectrum of $H_2C{=}S$,[9a,b] to our knowledge the study of thioacetone by that group[9c] has been the only other ab initio study to date of thioketone electronic spectra. It was therefore anticipated that our calculations should not only confirm the $n-\pi^*$ assignment of the long-wavelength transition but should also be able to resolve the question of the assignments of the two more energetic transitions lying in the 200–250-nm region of thioketone spectra.

Experimental Results and Discussion

Synthesis, Stereochemistry, and ^{13}C NMR. All thiones (**1**, **3**, and **5**) in this work were prepared by heating the parent substituted adamantanone in dry pyridine with phosphorus pentasulfide. The methyl ketones were prepared from the known (+)-*endo*-bicyclo[3.3.1]non-6-ene-3(*R*)-carboxylic acid (**7**), whose absolute configuration had been previously established.[26] Reaction of the lithium carboxylate of **7** with methyllithium gave ketone **8**, which upon reduction with $LiAlH_4$ (to give **9**) and subsequent solvolytic cyclization in hot formic acid[22] yielded the mixture of epimeric methyladamantanols (four isomers, **11**). Jones oxidation of **11** cleanly gave a separable mixture of **2** and **4**. The β-methyladamantanones prepared in this way were identical with those prepared earlier by Snatzke et al.[23] and in our laboratory.[22,24b] Dideuterioadamantanone **6** was prepared in a similar way from **7**, first by reduction of the methyl ester of **7** to dideuterio alcohol

(11) Engelbrecht, J. P.; Anderson, G. D.; Linder, R. E.; Barth, G.; Djerassi, C.; Seamans, L.; Moscowitz, A. *Spectrochim. Acta, Part A* **1975**, *31A*, 507–513 and references therein.
(12) Trabjerg, I.; Vala, M.; Baiardo, J. *Mol. Phys.* **1983**, *50*, 193–204.
(13) Djerassi, C.; Herbst, D. *J. Org. Chem.* **1961**, *26*, 4675–4677.
(14) Djerassi, C. "Optical Rotatory Dispersion"; McGraw-Hill: New York, 1960; pp 45, 47.
(15) Moffitt, W.; Woodward, R. B.; Moscowitz, A.; Klyne, W.; Djerassi, C. *J. Am. Chem. Soc.* **1961**, *83*, 4013–4018.
(16) Emeis, C. A.; Oosterhoff, L. J. *J. Chem. Phys.* **1971**, *54*, 4809–4819.
(17) (a) Numan, H.; Neuwese, F.; Wynberg, H. *Tetrahedron Lett.* **1978**, 4857–4858. (b) Numan, H.; Wynberg, H. *J. Org. Chem.* **1978**, *43*, 2232–2236.
(18) Schippers, P. H.; Dekkers, H. P. J. M. *Chem. Phys.* **1982**, *69*, 19–26.
(19) Bouman, T. D.; Lightner, D. A. *J. Am. Chem. Soc.* **1976**, *98*, 3145–3154.
(20) Ripperger, H. *Z. Chem.* **1977**, *17*, 250–258.
(21) Kirk, D. N. *J. Chem. Soc., Perkin Trans. 1* **1974**, 1076–1103.
(22) Lightner, D. A.; Wijekoon, W. M. D. *J. Org. Chem.* **1982**, *47*, 306–310.
(23) (a) Snatzke, G.; Ehrig, B.; Klein, H. *Tetrahedron* **1969**, *25*, 5601–5609. (b) Snatzke, G.; Eckhardt, G. *Ibid.* **1968**, *24*, 4543–4558. (c) Snatzke, G.; Eckhardt, G. *Chem. Ber.* **1968**, *101*, 2010–2027.
(24) (a) Lightner, D. A.; Jackman, D. E. *J. Am. Chem. Soc.* **1974**, *96*, 1938–1939. (b) Lightner, D. A.; Chang, T. C. *Ibid.* **1974**, *96*, 3015–3016.
(25) The magnitude has been called exceptionally large by Others: Barth G.; Djerassi, C. *Tetrahedron* **1981**, *24*, 4123–4142.
(26) Numan, H.; Troostvijk, C. B.; Wierenga, J. H.; Wynberg, H. *Tetrahedron Lett.* **1977**, 1761–1764.

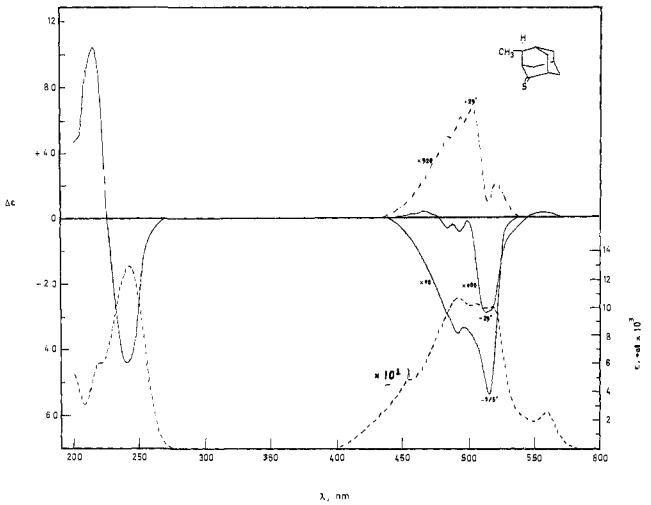

Figure 1. Circular dichroism spectra of thioketone **1** in *n*-heptane (---) at 26 °C, and in methylcyclohexane–isopentane (4:1) (—) at 26 °C and −175 °C, all corrected to 100% ee and for solvent contraction. The positive part of the 26 °C curve in methylcyclohexane–isopentane (4:1, v/v) carries the same scale as the major negative part. Ultraviolet–visible spectrum (---) in *n*-heptane at room temperature.

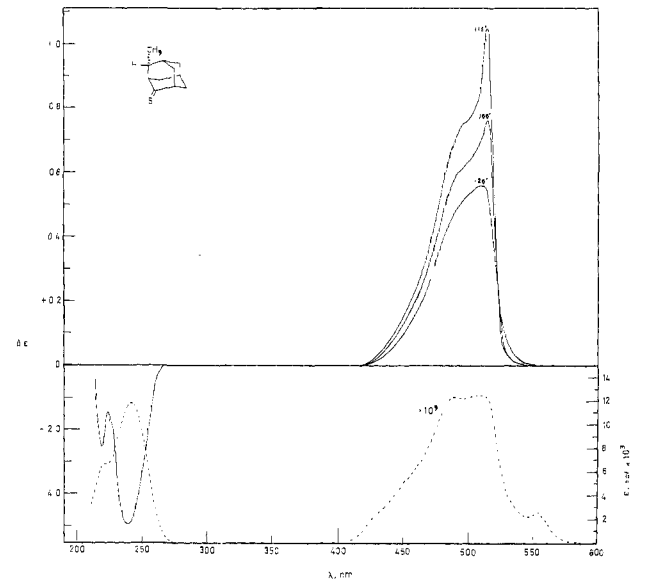

Figure 2. Circular dichroism spectra (—) of thioketone **3** in *n*-heptane at 26 °C and in methylcyclohexane–isopentane (4:1, v/v) at −100 °C and −175 °C, all corrected to 100% ee and for solvent contraction. Ultraviolet–visible spectra (---) of **3** in *n*-heptane at room temperature.

10, then solvolysis of **10** to form **12**, followed by Jones oxidation. The absolute configuration and enantiomeric excess (ee) of the ketones and thioketones follow from previous work with β-methyladamantanones.[17b,22,23,24b,27]

The ^{13}C NMR assignments for thioketones **1**, **3**, and **5** and their corresponding parent ketones **2**, **4**, and **6** are given in Table I. The ^{13}C NMR of dideuterio compounds **5** and **6** confirms the previous assignments made for adamantanone[28,29] and adamantanethione,[28] and we note that sulfur is a better internal shift reagent than oxygen and causes all of the ring carbons of adamantanethione

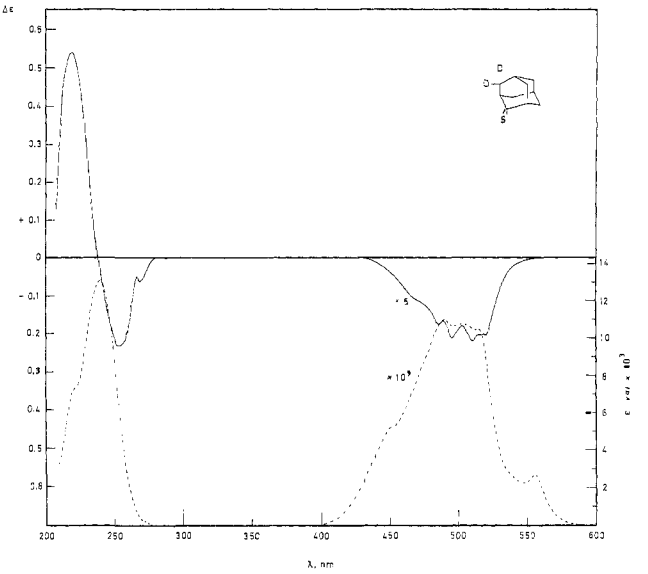

Figure 3. Circular dichroism (—) and ultraviolet–visible (---) spectra of thioketone **5** in *n*-heptane at room temperature. The CD spectrum is corrected to 100% ee.

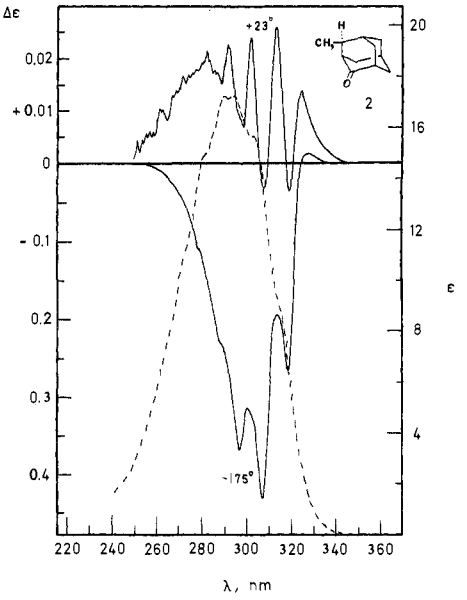

Figure 4. Circular dichroism spectra (—) of ketone **2** in methylcyclohexane–isopentane (4:1, v/v) corrected to 100% ee and for solvent contraction. Temperatures (°C) are indicated near the curves. Ultraviolet spectrum (---) of **2** at room temperature in the same solvent.

to be even more deshielded than their counterparts in adamantanone. The α-carbons (C-1 and C-3) are most strongly affected, whereas the one farthest removed (C-7) hardly changes.

The observed strong deshielding of the thioketone carbon (270 ppm) resonance relative to the carbonyl carbon (218 ppm) has been discussed earlier[28,30] in terms of bond polarization with a

(27) Both the ee and absolute configuration of **2** have been determined using the Mosher ester [Kalyanam, N.; Lightner, D. A. *Tetrahedron Lett.* **1979**, 415–418] of the derived *syn*-alcohol: Wijekoon, W. M. D.; Lightner, D. A., in preparation.

(28) Andrieu, C. G.; Debruyne, D.; Paquer, D. *Org. Magn. Reson.* **1978**, *11*, 528–531.

(29) (a) Loomes, D. J.; Robinson, M. J. T. *Tetrahedron* **1977**, *33*, 1149–1157. (b) Duddeck, H.; Wolff, P. *Org. Magn. Reson.* **1977**, *9*, 528–32. (c) Abraham, R. J.; Chadwick, D. J.; Griffiths, L. *Tetrahedron Lett.* **1979**, 4691–4694.

(30) Olah, G. A.; Nakajima, T.; Prakash, G. K. S. *Angew. Chem., Int. Ed. Engl.* **1980**, *19*, 811–812.

(31) Lightner, D. A.; Gawronski, J. K.; Bouman, T. D. *J. Am. Chem. Soc.* **1980**, *102*, 1983–1990.

(32) (a) Moscowitz, A.; Wellman, K. M.; Djerassi, C. *Proc. Natl. Acad. Sci. U.S.A.* **1963**, *50*, 799–804. (b) Kirk, D. N.; Klyne, W.; Wallis, S. R. *J. Chem. Soc. C* **1979**, 350–360. (c) Hayes, W. P.; Timmons, C. J. *Spectrochim. Acta* **1965**, *21*, 529–541.

(33) For a recent review, see: Oddershede, J. *Adv. Quantum Chem.* **1978**, *11*, 275–352.

(34) Hansen, Aa. E.; Bouman, T. D. *Adv. Chem. Phys.* **1980**, *44*, 545–644.

(35) Hansen, Aa. E.; Bouman, T. D., in preparation.

(36) This is convenient in the present context; however if information about directional charge-transfer effects is desired, the two terms in eq 8 should be retained separately.

Table I. Carbon-13 NMR Assignments for Adamantanones[a] and Adamantanethiones[b]

	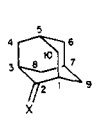		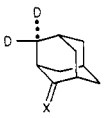		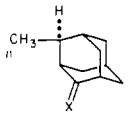		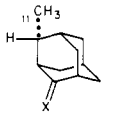	
C	X = O	X = S	X = O	X = S	X = O	X = S	X = O	X = S
1	46.76 (d)	57.62 (d)	46.70 (d)	58.01 (d)	46.64 (d)	57.66 (d)	45.82 (d)	57.39 (d)
2	217.88 (s)	269.09 (s)	218.23 (s)	271.20 (s)	217.64 (s)	269.52 (s)	217.70 (s)	270.96 (s)
3	46.76 (d)	57.62 (d)	46.87 (d)	58.17 (d)	53.13 (d)	63.51 (d)	51.90 (d)	63.39 (d)
4	39.03 (t)	41.25 (t)			43.07 (d)	44.64 (d)	39.91 (d)	42.49 (d)
5	27.22 (d)	27.76 (d)	27.33 (d)	28.07 (d)	32.83[c] (d)	32.71 (d)	32.36[c] (d)	32.98 (d)
6	36.05 (t)	36.72 (t)	36.17 (t)	36.97 (t)	37.63 (t)	38.17[c] (t)	29.61 (t)	30.56 (t)
7	27.22 (d)	27.76 (d)	27.16 (d)	27.91 (d)	26.80 (d)	27.17 (d)	27.26 (d)	27.99 (d)
8	39.03 (t)	41.25 (t)	39.09 (t)	41.56 (t)	39.50[d] (t)	42.22[d] (t)	32.01[c] (t)	34.62 (t)
9	39.03 (t)	41.25 (t)	39.09 (t)	41.56 (t)	39.32[d] (t)	41.91[d] (t)	38.97[d] (t)	41.71 (t)
10	39.03 (t)	41.25 (t)	39.09 (t)	41.56 (t)	33.59[c] (t)	35.63[c] (t)	39.15[d] (t)	41.71 (t)
11					18.50 (q)	18.67 (q)	16.80 (q)	17.78 (q)

[a] In $CDCl_3$ at 25 MHz (6000-Hz sweep width), using a deuterium lock on δ 77.0, values in ppm downfield from tetramethylsilane. [b] In CD_2Cl_2 at 25 MHz (8000-Hz sweep width), using a deuterium lock on δ 53.8, values in ppm downfield from tetramethylsilane. [c] Assignments may interchanged. [d] Assignments may be interchanged.

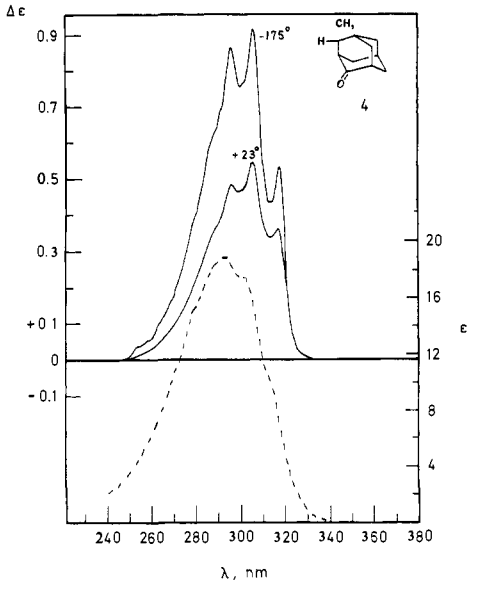

Figure 5. Circular dichroism spectra (—) of ketone **4** in methylcyclohexane–isopentane (4:1, v/v) corrected to 100% ee and for solvent correction. Temperatures (°C) are indicated near the curves. Ultraviolet spectrum (---) of **2** at room temperature in the same solvent.

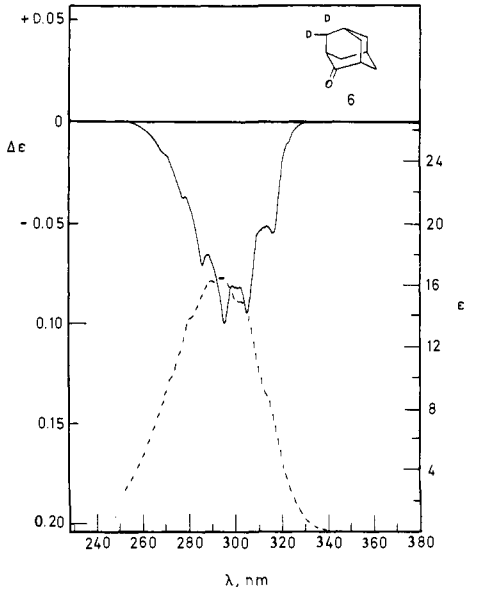

Figure 6. Circular dichroism (—) and ultraviolet (---) spectra of ketone **6** at room temperature. The CD spectrum is corrected to 100% ee.

greater positive charge character in the C=S carbon. However, this rationalization is not borne out by our calculations. In fact, the computed electron density is larger on the C=S carbon than on the C=O carbon by about 0.25 electron. It therefore appears more appropriate to ascribe the resulting increase in the deshielding in thiones to the combined effect of a *decrease* in the diamagnetic part of the deshielding (due to the higher electron density) and a significantly larger *increase* in the paramagnetic part (relative to a gauge origin within the chromophore).[45,46] The leading contribution to the paramagnetic term comes from the magnetic dipole allowed n–π* transition,[47] for which the lower excitation energy in C=S leads to the appropriate larger deshielding. This is in line with the almost linear correlation between ^{13}C chemical shift and n–π* excitation wavelength found in ketones.[48] (More quantitative studies of these screening effects will be reported in due course.)

Circular Dichroism. The CD and UV spectra of thiones **1**, **3**, and **5** are shown in Figures 1–3. The curves may be compared with those of the parent ketones **2**, **4**, and 6 of Figures 4–6. The thiones and ketones generally show strikingly similar behavior in the CD of their long-wavelength (n–π*) transitions: the equatorial-methyl isomers **3** and **4** both give (+) CEs in methylcyclohexane–isopentane with little change upon lowering the temperature; the axial-methyl isomers **1** and **2** both show a pro-

(37) Howell, J. M. *J. Chem. Phys.* **1970**, *53*, 4152–4160.
(38) Bendazzoli, G.; Biscarini, P.; Palmieri, P.; Gottarelli, G. *J. Chem. Soc., Faraday Trans 2* **1981**, *77*, 503–511.
(39) Akagi, K.; Yamabe, T.; Kato, H.; Imamura, A.; Fukui, K. *J. Am. Chem. Soc.* **1980**, *102*, 5157–5165.
(40) Murray, R. K., Jr.; Goff, D. L. *J. Org. Chem.* **1978**, *43*, 3844–3848.
(41) Eisenbraun, E. J. "Organic Synthesis"; Wiley: New York, 1973; Collect Vol. V, pp 310–314.
(42) Blaney, F.; Faulkner, D.; McKervey, M. A.; Step, G. *J. Chem. Soc., Perkin Trans. 1* **1972**, 2697–2701.
(43) (a) Binkely, J. S.; Whiteside, R. A.; Hariharan, P. C.; Seeger, R.; Pople, J. A.; Hehre, W. D.; Newton, M. D. *QCPE* **1978**, *11*, 368. Cook, C. M. *Ibid* **1981**, *13*, 391. (b) Hehre, W. J.; Stewart, R. F.; Pople, J. A. *J. Chem. Phys.* **1969**, *51*, 2657–2664. (c) Ditchfield, R.; Hehre, W. J.; Pople, J. A. *Ibid* **1971**, *54*, 724–728. Hehre, J.; Lathan, W. A. *Ibid.* **1972**, *56*, 5255–5257.
(44) Bouman, T. D.; Hansen, Aa. E.; Voigt, B.; Rettrup, S. *Int. J. Quantum Chem.* **1983**, *23*, 595–611. *QCPE Bull.* **1983**, *3*, 63, Program QCPE 459.
(45) Carrington, A.; McLachlan, A. D. "Introduction to Magnetic Resonance"; Harper and Row: New York, 1967.
(46) Gunther, H. "NMR Spectroscopy"; Wiley: New York, 1973.
(47) Tokuhiro, T.; Appleman, B. R.; Fraenkel, G.; Pearson, P. K.; Kern, C. W. *J. Chem. Phys.* **1972**, *57*, 20–28.
(48) Savitsky, G. B.; Namikawa, K.; Zweifel, G. *J. Phys. Chem.* **1965**, *69*, 3105–3109.

Table II. Experimental n–π* Rotatory Strengths[a] for Thioadamantanones and Adamantanones, Measured at Room Temperature

compd	solvent	λ_{max}	R
1 (β-ax, thione)	*n*-heptane (I)	504.5[b]	+0.061[a]
	MI 4:1 (II)[c]	514	−0.026
	perfluoro-pentane (III)	507.5	+0.19
	p-dioxane (IV)	505	−0.25
2 (β-ax, ketone)	I	299.5	+0.089
	II	312.5	+0.073
	III	305.5	+0.085
	IV	303.5	−0.19
3 (β-eq, thione)	I	516	+1.21
	II	512	+1.41
	III	518	+1.19
	IV	499.5	+1.53
4 (β-eq, ketone)	I	304	+1.58
	II	305	+1.43
	III	303.5	+1.78
	IV	301.5	+2.09
5 (thione)	I	508	−0.105
	IV	500	−0.113
6 (ketone)	I	295	−0.250
	IV	294	−0.281

[a] Rotatory strength, R: (cgs) × 10^{40}. [b] Wavelength in nanometers. [c] MI 4:1 = methylcyclohexane–isopentane 4:1 (v/v).

nounced temperature effect on highly structured, essentially (−) CEs.[22] In addition, thioketone **1** exhibits oppositely signed long-wavelength CEs in two different hydrocarbon solvents at room temperature: (+) in *n*-heptane and (−) in methylcyclohexane–isopentane (4:1, v/v); whereas the parent ketone **2** shows no sign change in these solvents. At low temperatures (0 to −78 °C) in *n*-heptane, **1** exhibits the expected (−) long-wavelength CE, and the short-wavelength bands exhibit the same CE signs and magnitudes in the various solvents.

The close correlation between thioketone and ketone long-wavelength CD Cotton effects exhibited by **1–4** adds weight to the prior evidence[4] that these electronic transitions are essentially of the same n–π* character, and the hypsochromic shift of the CD and UV bands in going from *n*-heptane to *p*-dioxane solvents supports this conclusion (Table II).[4] Furthermore, the relatively strong consignate CEs observed for the 3-equatorial methyl group of **3** and **4**, and their modest[22,23,32] solvent dependence (Table II), indicate that the classical octant rule[15] obtains for this well-studied position, even in cyclohexanethione systems. The dissignate CEs observed for the 3-axial methyl group of **1** and **2** are in accord with the updated octant rule[19] as applied to cyclohexanethiones. With respect to the latter, the third nodal surface[15,19] associated with the C=S group, in analogy to the C=O group, expectedly places the axial methyl group in an upper left (or lower right) front octant in both **1** and **2**. This proximity of the perturber to a nodal surface provides a ready rationale for the pronounced solvent and temperature effects. For the ketone, solvent-induced CE sign changes are well established.[22,23] The perfluoropentane values might be presumed to represent "unsolvated" gas-phase values.

Thioketone **5** and its parent ketone **6** both exhibit (−) n–π* CEs in keeping with the previously noted dissignate behavior of deuterium as an octant perturber.[31] Our CD spectrum of **5** agrees with the spectrum recently reported by Schippers and Dekkers,[18] and we assume, as they do, that an error in scale is responsible for an earlier claim that the CD spectra of **5** and **6** should differ by an order of magnitude.[17a]

The region between 200 and 250 nm shows two bands in the UV of **1**, **3**, and **5**: an intense peak at about 245 nm and a weaker one (shoulder) at about 217 nm.[4b] Two bands are clearly visible in the CD spectra of the thioketones in the same region. The peak positions of the bands of **1** ($\Delta\epsilon_{215}^{max}$ +10.5 and $\Delta\epsilon_{240}^{max}$ −4.4) and **3** correspond closely with those of the UV bands; the shorter wavelength CD band, however, is (+) for **1** and (−) for **3**. Similarly (−)-thiofenchone exhibits oppositely signed CD transitions at $\Delta\epsilon_{242}^{max}$ −8.57 and $\Delta\epsilon_{220}^{max}$ +3.80.[6] In **5**, the longer wavelength CD band is displaced by about 10 nm to the red side of the UV band, while the other band (+) corresponds closely to the UV peak position. In all three cases, the CE at ca. 245 nm is (−).

Calculation of Low-Lying Excitations

A detailed understanding of electronic excitation energies and intensities requires a theoretical treatment that goes beyond the orbital level of approximation and that includes electron correlation effects. We have found the random-phase approximation (RPA) method[33] to be capable of providing a balanced treatment of electron correlation effects on chiroptical properties that is difficult to achieve at feasible levels of ordinary configuration interaction.[34]

The reader is referred elsewhere for a detailed discussion of the RPA method.[33,34] Briefly, the excitation energies ΔE_{0q} for transitions from the ground state 0 to low-lying excited states q are determined by solving the coupled set of equations:

$$\sum_{(l'm')} \{A_{(lm),(l'm')}X_{(l'm'),q} + B_{(lm),(l'm')}Y_{(l'm'),q}\} = \Delta E_{0q}X_{(lm),q} \quad (1a)$$

$$\sum_{(l'm')} \{B_{(lm),(l'm')}X_{(l'm'),q} + A_{(lm),(l'm')}Y_{(l'm'),q}\} = -\Delta E_{0q}Y_{(lm),q} \quad (1b)$$

where the indices (lm), $(l'm')$ refer to the singly excited configurations obtained, respectively, by promoting an electron from occupied orbital l to unoccupied orbital m, and from l' to m′. The matrix elements $A_{(lm),(l'm')}$ and $B_{(lm),(l'm')}$ are defined as $\langle l \rightarrow m|\hat{\mathcal{H}} - E_0|l' \rightarrow m'\rangle$ and $\langle \Delta_0|\hat{\mathcal{H}}|l \rightarrow m, l' \rightarrow m'\rangle$, respectively, where E_0 and Δ_0 are the closed-shell, self-consistent single-determinant ground-state energy and wave function, respectively. The coefficients $X_{(lm),q}$ and $Y_{(lm),q}$ are used to determine the transition moments for spin singlet excitations as follows:[34]

electric dipole length

$$\langle 0|r|q\rangle = \sqrt{2}\sum_{(lm)} \{X_{(lm),q} + Y_{(lm),q}\}\langle l|r|m\rangle \quad (2a)$$

electric dipole velocity

$$\langle 0|\hat{\nabla}|q\rangle = \sqrt{2}\sum_{(lm)} \{X_{(lm),q} - Y_{(lm),q}\}\langle l|\hat{\nabla}|m\rangle \quad (2b)$$

magnetic dipole

$$\langle 0|r \times \hat{\nabla}|q\rangle = \sqrt{2}\sum_{(lm)} \{X_{(lm),q} - Y_{(lm),q}\}\langle l|r \times \hat{\nabla}|m\rangle \quad (2c)$$

The X and Y coefficients obey orthonormality and closure relations that are discussed elsewhere.[33,34]

Of the various expressions available for calculating the overall oscillator and rotatory strengths,[34] we will make use of the following in this paper (in cgs units):

$$f_{0q}^{\nabla} = (2\hbar^2/3m\Delta E_{0q})|\langle 0|\hat{\nabla}|q\rangle|^2 \quad (3a)$$

$$f_{0q}^{\nabla} = \tfrac{2}{3}\langle 0|\hat{\nabla}|q\rangle \cdot \langle 0|r|q\rangle \quad (3b)$$

$$R_{0q}^{\nabla} = (e^2\hbar^3/2m^2c\Delta E_{0q})\langle 0|\hat{\nabla}|q\rangle \cdot \langle 0|r \times \hat{\nabla}|q\rangle \quad (3c)$$

$$R_{0q}^{[r]} = R_{0q}^{\nabla}(f_{0q}^{r\nabla}/f_{0q}^{\nabla}) \quad (3d)$$

Equation 3d defines the origin-independent part of the dipole length form R_{0q}^{r} of the rotatory strength; R_{0q}^{r} itself depends in general on the choice of origin of the coordinate system.[34] Note that $R_{0q}^{[r]}$, like f_{0q}^{∇}, has no explicit dependence on the excitation energy, so that errors in the calculation of ΔE_{0q} do not affect the computed intensities in these forms.[34]

n → π* transitions are usually considered well characterized as valence shell excitations; however since we aim at addressing also the nature of the higher excitations and since extended atomic basis sets are commonly prescribed for sulfur-containing systems, we present in Tables III and IV the results of a number of RPA calculations on thioacetone ($(CH_3)_2C{=}S$) and methyl ethyl thioketone (2-butanethione, $CH_3(CS)C_2H_5$), the latter held in a chiral conformation such that C-4 occupies a position in the upper left back octant (cf. compound V in ref 19). Three basis sets were used: (A) minimal, (B) split valence, and (C) split valence plus

Table III. Comparison of Calculations of the Low-Lying Excitations of Thioacetone Using Basis C with Other Calculations and with Experiment

state	this work	ref 8c	exptl[a]
$^3A_2$ n-π^*	2.34[b]	2.18	2.12[c]
$^1A_2$ n-π^*	3.04	2.53	2.48
$^1A_1$ π-π^*	5.60	7.19	5.3
$^1B_2$ n-4s (σ^*)	6.22	5.23	5.82
$^1B_1$ σ-π^*	6.51	7.10	
$^1B_2$ n-4p$_\sigma$	6.89	5.93	
$^1A_2$ n-4pb$_1$	6.97	5.90	
$^1A_1$ n-4pb$_2$	7.21	6.04	
$^1B_1$ π-σ^*	7.28	6.80, 7.78	

[a] Reference 4b, given for di-*n*-propyl thioketone. [b] Calculated in TDA (monoexcited CI). [c] Reference 11.

Table IV. Summary of RPA Calculated Chiroptical Properties of the Lowest Three States of Thioacetone (THA) and Methyl Ethyl Thioketone (MET)

molecule	basis	state	assignment	ΔE[a]	f^{v}	R^{v} [b]	$R^{[r]}$ [b]
THA	A	1	n-π^*	2.68	$<10^{-3}$	0	0
		2	σ_{CS}-π^*	6.39	0.012	0	0
		3	π-π^*	6.47	0.127	0	0
	B	1	n-π^*	3.15	$<10^{-3}$	0	0
		2	π-π^*	5.84	0.194	0	0
		3	σ_{CS}-π^*	6.34	0.005	0	0
	C	1	n-π^*	3.05	$<10^{-3}$	0	0
		2	π-π^*	5.60	0.260	0	0
		3	n-4s	6.22	0.095	0	0
		(4	σ_{CS}-π^*	6.51	0.003	0	0)[c]
MET	A	1	n-π^*	2.68	$<10^{-3}$	2.3	2.5
		2	σ_{CS}-π^*	6.34	0.020	−8.2	−8.5
		3	π-π^*	6.45	0.126	4.0	9.2
	B	1	n-π^*	3.15	$<10^{-3}$	2.3	2.5
		2	π-π^*	5.81	0.207	−9.4	−0.6
		3	σ_{CS}-π^*	6.30	0.004	−11.3	−12.6
	C	1	n-π^*	3.04	$<10^{-3}$	2.9	1.8
		2	π-π^*	5.58	0.282	−0.2	−0.3
		3	n-4s	6.24	0.091	−2.9	−2.9
		(4	σ_{CS}-π^*	6.45	0.002	−13.4	−6.2)[c]

[a] Energies in eV. [b] (cgs) × 10^{40}. [c] Included for comparison.

a double set of d-type gaussian functions on sulfur and a single set of diffuse s and p Gaussian functions each on the thiocarbonyl C and S. The d orbitals on sulfur are added to account for the greater polarizability of the sulfur atom and for possible effects of low-lying 3d orbitals on the spectrum, while adding diffuse functions to the thiocarbonyl chromophore should account for low-lying Rydberg-type transitions. The calculation in basis C is intended to provide an "upper limit" to the reliability of the present set of calculations. Details of the computations and basis sets are presented in the Experimental Section. The set of single excitations in the RPA calculations comprised all excitations from the valence SCF-MOs into the virtual orbitals. (Sulfur 2s and 2p orbitals are included in the "core"; a test calculation on thioacetone showed that they do not contribute significantly to the low-lying excitations.) The effects of the corresponding, much larger set of double excitations are included automatically in the RPA.[34]

In Table III the present results for thioacetone are compared to the results of the extensive CI calculations of Peyerimhoff et al.[9c] and with experiment.[4b] They compare quite favorably, and in fact our computed π-π^* excitation energy is closer to experiment. No attempt was made to optimize the exponents of the diffuse basis functions dominating the Rydberg-type excitations. The results for thioacetone and for the achiral conformation of methyl ethyl thioketone are shown in Table IV. Experimentally, the weak band in the UV of thiones extends from about 2.2 to 3.2 eV, and the two stronger bands extend from about 4.5 to 6 eV. Our calculated energies are at the high ends of these ranges, by a few tenths of an electronvolt, as is characteristic of truncations of the atomic orbital basis. We identify the long-wavelength band as the n-π^* transition, as expected, and the second band as π-π^*, for reasons discussed below. (These designations refer only to the leading component in the mixture of primitive excitations defining the overall transition.) The assignment of the third band is less certain. In the minimal basis set (basis A), the second lowest excitation is σ_{CS}-π^* (where σ_{CS} is the bonding σ orbital between C and S), occurring at about 6.4 eV. As the basis set is expanded, however (bases B and C), the π-π^* excitation moves down in energy, ending up around 5.6 eV in basis C. The nature of what has now become the third band changes: from an essentially valence-like, σ-π^* excitation, the transition becomes largely diffuse in nature, essentially n-4s. (Although as pointed out earlier,[9c] whether one designates such a transition as n-4s or n-σ^* is largely a matter of taste.) A valence-like, n-σ^* transition is predicted to occur at much highr energies (≥10 eV) by the smaller basis sets. Our calculations indicate that the σ_{CS}-π^* excitation should occur quite close to the n-4s, so that the observed band in this region might well have substantial valence character, particularly in solution. Note that the excitation energies do not change monotonically as the basis set is expanded—nor should they be expected to, since the variation principle does not apply to transition properties—but the overall agreement with the observed spectrum improves.

In the chirally disposed methyl ethyl thioketone we are able in addition to predict the CD spectrum. We compute the rotatory strength $R^{[r]}$ (eq 3d) of the n-π^* transition to be about 2×10^{-40} cgs, relatively independent of the basis set, and in accord with the prediction of the octant rule for the α-axial position.[15,19] The second band is predicted to be negative, and the magnitude of the negative CE in the 6-eV region increases as the basis set is expanded. Note that, while basis A predicts a positive rotatory strength for π-π^*, that transition acquires negative rotatory strength as it moves lower in energy. In both model compounds, we compute a red shift of about 0.85 eV for the π-π^* excitation as the basis set is improved, while the n-π^* and σ_{CS}-π^* bands remain essentially constant.

We feel confident that the properties of the long-wavelength band (n-π^*) are well represented in all three atomic orbital bases and that basis C can give an adequate description of the optical properties in the entire $\lambda \geq 200$ nm spectral region. However, the congestion of excitations in the 200–250-nm region apparently cannot be reliably resolved in minimal or split-valence basis sets.

Armed with this experience on model compounds, we performed minimal basis-set RPA calculations on the methyladamantanone and thione derivatives **1–4**; the size of these molecules precludes the use of extended basis sets. For **4** only the fully staggered methyl conformation was considered, whereas both staggered and eclipsed methyl conformations were considered for **1–3** in order to assess the sensitivity of the n-π^* chiroptical properties to a change in rotamer conformation. The deuterio compounds **5** and **6** were not treated because of our primary interest in studying the role of the alkyl substituents in thioketone octant rule behavior. The results are shown in Table V.

For the n-π^* transition, the agreement with the experimental results is very good, with regard both to energies and to sign and magnitude of the rotatory strengths. The computed chiroptical properties for the thioketones and ketones are very similar, and the revised octant rule[19] is obeyed in all cases. In particular, the proximity of the β-axial methyl group to a nodal surface is reconfirmed by the sensitivity of the rotatory strength of **1** and **2** to rotamer conformation. This behavior was not observed in our earlier CNDO/S results for **2**, in which only the single n-π^* configuration was used to describe the lowest excitation.[22] These results suggest that the very pronounced temperature and solvent effects in the CD in **1** and **2** are at least as strongly determined by restricted rotation of the methyl group as by solvent perturbation of the C=S chromophore or by vibronic effects.[22]

For the π-π^* transition a "basis-set correction" of 0.85 eV as found above in methyl ethyl ketone brings this transition into fair agreement, in terms of energy and oscillator strength, with the strong ordinary absorption band in **1** and **3** at about 240 nm. We note also that this transition is computed to carry a negative

Table V. Summary of Computed (STO4G-RPA) Chiroptical Properties for Compounds 1–4

compd	state	ΔE, eV	$f^{r\nabla}$	$R^{[r]}$ [a]	R^{∇} [a]	λ_{max}, nm
1 (staggered)	n–π^*	2.75	$<10^{-3}$	−0.2	−0.3	451
	π–π^*	5.60[b]	0.14	−2.6	−1.4[b]	221
	σ–π^*	6.42	0.04	+2.5	+1.6	193
1 (eclipsed)	n–π^*	2.75	$<10^{-3}$	+0.1	+1.0	450
	π–π^*	5.60[b]	0.15	−2.6	−1.3[b]	220
	σ–π^*	6.42	0.02	−0.6	−0.5	193
2 (staggered)	n–π^*	4.29	$<10^{-3}$	−0.3	−0.4	289
	σ–π^*	8.98	0.001	+0.03	+0.4	138
	π–π^*	9.80[b]	0.17	−0.3	−0.1[b]	126[b]
2 (eclipsed)	n–π^*	4.29	$<10^{-3}$	+0.2	+0.6	289
	σ–π^*	8.98	0.001	−0.1	−1.8	138
	π–π^*	9.80[b]	0.17	+1.5	+0.9[b]	126[b]
3 (staggered)	n–π^*	2.76	$<10^{-3}$	+1.3	+0.8	450
	π–π^*	5.61[b]	0.16	+4.8	+2.5[b]	221[b]
	σ–π^*	6.43	0.02	−8.2	−7.3	193
3 (eclipsed)	n–π^*	2.76	$<10^{-3}$	+1.3	+0.8	450
	π–π^*	5.61[b]	0.16	+4.4	+2.3[b]	221
	σ–π^*	6.43	0.02	−9.1	−7.6	193
4 (staggered)	n–π^*	4.30	$<10^{-3}$	+1.7	+1.2	289
	σ–π^*	8.98	0.002	−0.4	−4.9	138
	π–π^*	9.81[b]	0.19	−0.5	−0.3[b]	126[b]

[a] Units are (cgs) × 10^{40}. [b] Derived by subtracting 0.85 eV from computed energy (see text).

rotatory strength in all but the smallest basis set, in agreement with the negative second band observed in **1**, **3**, and **5**. However as cautioned above, for these molecules the minimal basis set does not seem sufficient to provide reliable rotatory strengths in this spectral region. Since these spectra are recorded in condensed phase, a valence-type assignment (σ–π^* or π–π^*, Table V) for the second band in the 200–250-nm region appears more likely than the n–4s Rydberg excitation which could be expected from the basis C results in Table IV.

Analysis of Computed Intensities

In order to extract more structural information from the computed excitation properties than is apparent from the overall results, we have analyzed the rotatory strengths for the n–π^* excitations in terms of atom and bond contributions. The method is described in detail elsewhere;[35] we present only a brief summary here, and for reasons given in ref 35 we use only the dipole velocity form of the rotatory strength R^{∇}_{0q}, eq 3c, in this analysis. In what follows we denote atomic orbitals by μ, ν, occupied (virtual) molecular orbitals by l(m), and atoms by A, B, C, D. Expanding the molecular orbitals in the form

$$\phi_l = \sum_\mu \chi_\mu C_{\mu l} \qquad \phi_m = \sum_\nu \chi_\nu C_{\nu m} \tag{4}$$

the matrix elements in eq 2b,c become

$$\langle 0|\hat{\nabla}|q\rangle = \sqrt{2}\sum_\mu\sum_\nu \langle\mu|\hat{\nabla}|\nu\rangle \sum_l\sum_m \{X_{lm,q} - Y_{lm,q}\} C_{\mu l} C_{\nu m} \equiv \sum_\mu\sum_\nu \langle\mu|\hat{\nabla}|\nu\rangle \Lambda_{\mu\nu,q} \tag{5}$$

and similarly

$$\langle 0|r \times \hat{\nabla}|q\rangle = \sum_\mu\sum_\nu \langle\mu|r \times \hat{\nabla}|\nu\rangle \Lambda_{\mu\nu,q} \tag{6}$$

From these expressions we can define an effective atomic electric dipole velocity element for the total excitation 0 → q:

$$\nabla^{(q)}_{(A,A)} = \sum_{\mu>\nu}^{(A)} \langle\mu|\hat{\nabla}|\nu\rangle \{\Lambda_{\mu\nu,q} - \Lambda_{\nu\mu,q}\} \tag{7}$$

and a bond element

$$\nabla^{(q)}_{(A,B)} = \sum_\mu^{(A)}\sum_\nu^{(B)} \langle\mu|\hat{\nabla}|\nu\rangle \{\Lambda_{\mu\nu,q} - \Lambda_{\nu\mu,q}\} \qquad A > B \tag{8}$$

where we have utilized the antihermitian character of the $\hat{\nabla}$ operator. The bond element in eq 8 therefore does not distinguish between A → B and B → A charge-transfer contributions.[36] For the magnetic dipole transition moment, atom and bond contributions are defined analogously. In terms of these contributions the rotatory strength becomes

$$R^{\nabla}_{0q} = (e^2\hbar^3/2m^2c\Delta E_{0q}) \sum_{A\geq BC\geq D} \sum \nabla^{(q)}_{(A,B)}\cdot(r \times \nabla)^{(q)}_{(C,D)} \tag{9}$$

which can also be written as

$$R^{\nabla}_{0q} = \sum_{A\geq BC\geq D} \sum R^{(q)}_{AB,CD} \tag{10}$$

where

$$R^{(q)}_{AB,CD} = (e^2\hbar^3/2m^2c\Delta E_{0q}) \times \tfrac{1}{2}\{\nabla^{(q)}_{(A,B)}\cdot(r \times \nabla)^{(q)}_{(C,D)} + \nabla^{(q)}_{(C,D)}\cdot(r \times \nabla)^{(q)}_{(A,B)}\} \tag{11}$$

The total dipole velocity rotatory strength R^{∇}_{0q} is origin invariant. However, the magnetic dipole moment elements $(r \times \nabla)^{(q)}_{(A,B)}$ are not invariant, and for (A,B) ≠ (C,D) the numerical values of the individual terms $\nabla^{(q)}_{(A,B)}\cdot(r \times \nabla)^{(q)}_{(C,D)}$ in eq 9 therefore depend in general on the origin chosen for molecular coordinate system. On the other hand, the symmetrization of the terms in eq 11 ensures that $R^{(q)}_{AB,CD}$ is in fact origin independent, because the origin dependence in the two terms cancels exactly,[35] as first pointed out by Howell.[37] A similar grouping of terms has been employed by Bendazzoli et al.[38] although without specific reference to the origin dependence problem, whereas the configuration interaction analysis of optical rotatory power presented recently by Akagi et al.[39] apparently overlooks this problem. The consequence of these observations is that one cannot, in general, separate the electric and magnetic dipole contributions to the total rotatory strength in a physically meaningful way.[35]

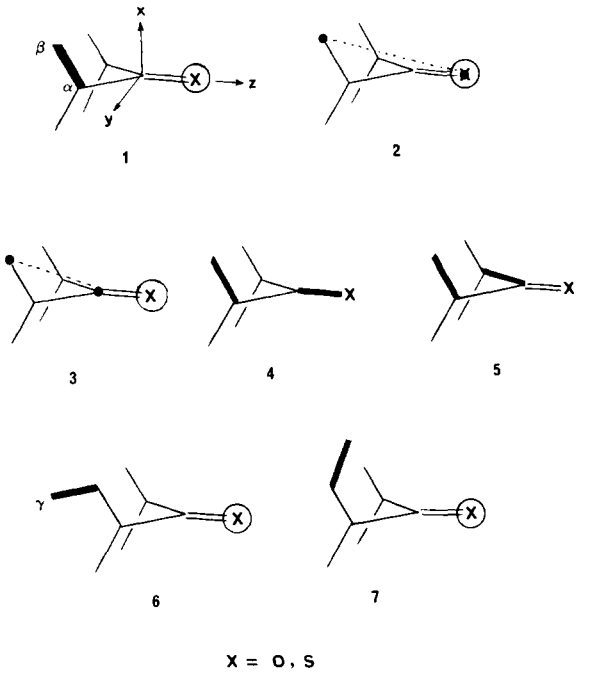

Figure 7. Coupling types ($R_{AB,CD}$) defined in text. A circled atom means that (A, B) or (C, D) is a one-center term, while a dashed line means that the atom pair (A, B) or (C, D) is not bonded. Bonded atom pairs entering the coupling term are indicated by heavy lines. Coupling types are illustrated only for quadrant 1 (Table VI).

Model Compounds. Let us consider first the model compounds thioacetone (THA) and methyl ethyl thioketone (MET). The leading contributions to the atom and bond decompositions, $R^{(q)}_{AB,CD}$ (eq 11), for the n–π^* rotatory strengths in these molecules are shown in Table VI and in Figure 7.

The five coupling types shown for THA and MET in Table VI and Figure 7 are significantly larger than all other couplings. Their numerical values vary somewhat with the basis set, but their relative importance is essentially unchanged. By far the largest coupling is the one between the α-axial bond and the sulfur atom

Table VI. Major Coupling Terms $R_{AB,CD}$ (eq 11) for the n–π^* Excitation in Thioacetone (THA) and Methyl Ethyl Thioketone (MET)

coupling type[a]	quadrant[b]	basis A[c]		basis B[c]		basis C[c]	
		MET[d]	THA	MET[d]	THA	MET[d]	THA
1	I	−13.74[e]	−17.84	−41.43	−48.10	−42.51	−47.67
	II	16.84	17.84	43.35	48.10	43.15	47.67
	III	17.90	17.84	46.86	48.10	49.37	47.67
	IV	−17.97	−17.84	−48.60	−48.10	−50.06	−47.67
2	I	2.31	3.03	6.89	8.77	10.78	13.69
	II	−2.93	−3.03	−8.55	−8.77	−11.05	−13.69
	III	−3.02	−3.03	−8.54	−8.77	−16.12	−13.69
	IV	3.02	3.03	8.88	8.77	13.46	13.69
3	I	5.76	4.02	26.26	17.90	23.11	15.10
	II	−4.01	−4.02	−15.54	−17.90	−16.37	−15.10
	III	−4.08	−4.02	−17.32	−17.90	−12.87	−15.10
	IV	4.02	4.02	17.31	17.90	15.45	15.10
4	I	3.11	3.25	15.89	18.26	23.44	24.00
	II	−3.08	−3.25	−16.55	−18.26	−23.94	−24.00
	III	−3.25	−3.25	−17.74	−18.26	−26.46	−24.00
	IV	3.28	3.25	18.61	18.26	27.88	24.00
5	I	−1.90	−2.60	−16.71	−21.93	−13.31	−16.62
	II	2.41	2.60	19.75	21.93	14.64	16.62
	III	2.59	2.60	21.49	21.93	17.06	16.62
	IV	−2.61	−2.60	−22.38	−21.93	−17.09	−16.62

[a] (A, B), (C, D) pairs for coupling types (Figure 7): 1, (C_α, β), (S, S); 2, (β, S), (S, S); 3, (C_S, β), (S, S); 4, (C_α, β), (C_S, S); 5, (C_α, β), (C_S, $C_{\alpha'}$). [b] Quadrant definitions: (I) +X, +Y; (II) −X, +Y; (III) +X, −Y; (IV) −X, −Y. Coordinate system as in ref 19 (see also Figure 7). [c] See text for basis set definitions. [d] The α-axial methyl is in quadrant I. The corresponding terms are grouped into a single term. [e] Units are (cgs) × 10^{40}.

one-center term (type 1). Remarkably, the sign pattern exhibited by the set of four equivalent couplings of type 1 is *dissignate*[21] with respect to the normal octant rule. That is, the coupling between the sulfur atom and the α-axial bond in the upper left back octant is *negative*, in contrast to the normal positive sign associated with this region. The remaining four coupling types that have the largest magnitudes are rather closely grouped in relative strength. They are, respectively, a nonbonded two-center interaction between the α-axial atom and the sulfur atom, coupled to the sulfur atom (type 2); a similar nonbonded interaction involving the β-axial atom–thiocarbonyl carbon pair and the sulfur atom (type 3); the coupling between the α–β (C–H or C–C) bond and the C=S bond (type 4); and finally, the coupling between the α–β bond and the in-plane (C_α–C) bond lying across the *X*–*Z* plane (type 5). Note that types 2–4 are all consignate couplings, while type 5 is dissignate.

In the chiral system MET, the five couplings described above exhibit dissymmetry in varying degrees across the local symmetry planes of the chromophore. In Table VI we display these terms grouping all terms involving the dissymmetric CH_3 group together in each case. For type 1 terms, we see that the net effect of the CH_3 group is to reduce the size of the strongly dissignate term in its quadrant, thus destroying the cancellation of terms across symmetry planes and leading to a net *consignate* effect. Similarly, the inherently consignate type 3 coupling is increased by the methyl group, while the other three types are reduced in magnitude. Other couplings (not shown), notably nonbonded interactions between the methyl group and the C=S bond and nonequivalent (C—C_α)–(C=S) couplings, act in a dissignate way to reduce the overall rotatory strength. It is interesting that basis sets B and C, which contain increasingly diffuse atomic orbitals, lead to numerically much larger coupling terms than the minimal basis A, while the net resulting intensities, Table IV, are essentially unchanged in the three bases.

It seems fair to say that the principal effect of an α-axial methyl perturber is to reduce the dissignate type 1 coupling while at the same time enhancing the consignate type 3 coupling, pointing to a through-bond mechanism. The analogy between these results and our earlier analysis of the electric dipole transition moment in ketones[19] is actually quite close. This suggests that, in the particular case of an electric-dipole-forbidden n–π^* transition strongly dominated by a local orbital promotion, the inherent origin dependence of the terms $\nabla_{AB}\cdot(^{o}r \times \nabla)_{SS}$ occuring in types 1–3 is in fact small, so that a discussion in terms of a coupling between a local magnetic moment on S with electric dipole moments involving the substituent groups is not totally out of place. It should be emphasized, however, that such a breakdown can safely be attempted only after the important origin-independent terms have been identified and the effects of an origin shift on the separate parts $\nabla_{AB}\cdot(r \times \nabla)_{CD}$ and $\nabla_{CD}\cdot(r \times \nabla)_{AB}$ (eq 11) have been assessed.

Methyladamantanethiones and Methyladamantanones. The foregoing analysis holds in large part also for compounds **1–4**. The principal coupling types are the same as types 1–5 above, with the exception that type 2 couplings diminish in importance and the couplings between the C_β–β_{eq} bonds and the sulfur atom ("type 6") appear instead. The results for **1–4** (with both methyl groups in staggered position) are displayed in Table VII, according to the four quadrants around the chromophore. Contributions involving the β-methyl perturber (quadrant I) are grouped into a single term for each coupling type. In the equatorially substituted **3** and **4** most of the dissymmetry is induced in type 1 and type 6 couplings. As before, the type 1 couplings are inherently dissignate, but the effect of the methyl substituent is to reduce the magnitude of the one in quadrant I, thus yielding a net consignate effect. The type 6 coupling involving the C_β–β_{eq} bond is inherently consignate, and the methyl perturber enhances it. A consignate term involving the coupling between the substituted C_β and S also appears, while the other large couplings show no substantial dissymmetry. The interactions shown in Table VII for **1** and **2** indicate little dissymmetry, with the exception of a "type 7" coupling between (C_β–β_{ax}) and sulfur. This coupling is small in general but contains most of the net rotatory strength for **1** and **2**. The type 7 coupling is dissignate, and the numbers shown in Table VII include a substantial (−0.56) contribution from the methyl carbon. In **3** and **4**, the type 7 couplings have a magnitude of 0.60 (0.50) and show almost no dissymmetry.

Since the overall results in Table V show that the n–π^* rotatory strength of **1** is very sensitive to small conformational changes, we compared the atom and bond contributions for (**1**, staggered) and (**1**, eclipsed). We found that rotating the methyl group changes all couplings (with S) along the chain of bonds from the methyl group to the sulfur atom, suggesting again that the effect is primarily due to a through-bond mechanism.

Finally, we compared the analyses of the n–π^* rotatory strength of **1** and **3** with the corresponding ketones **2** and **4**. The magnitudes of the couplings are consistently smaller in the ketones than the corresponding ones in the thioketones, but the induced dissymmetries are comparable, leading to essentially the same overall rotatory strengths in thioketones as in ketones. Moreover,

Table VII. Major $R_{AB,CD}$ Couplings for the n–π* Excitation in Compounds 1–4, with the Methyl Group in a Staggered Position[a]

coupling type	quadrant I	II	III	IV
		1 (Axial)		
1	−14.23	14.51	14.52	−14.65
2	4.55	−4.45	−4.44	4.47
4	2.67	−2.73	−2.73	2.75
5	−1.96	2.03	2.02	−2.05
6[b]	2.79	−2.86	−2.72	2.84
7[b]	−1.61	0.62	0.67	−0.64
		2 (Axial)		
1	−12.62	12.93	12.94	−13.07
2	0.56	−0.58	−0.57	0.58
3	3.85	−3.87	−3.88	3.89
4	3.25	−3.34	−3.34	3.36
5	−2.20	2.33	2.33	−2.36
6[b]	3.44	−3.58	−3.44	3.57
7[b]	−1.63	0.53	0.58	−0.53
		3 (Equatorial)		
1	−14.11	14.53	14.37	−14.49
2	4.38	−4.40	−4.42	4.47
4	2.66	−2.74	−2.70	2.72
5	−1.96	2.04	2.00	−2.03
6[b]	3.42	−2.85	−2.77	2.79
7[b]	−0.60	0.60	0.60	−0.60
		4 (Equatorial)		
1	−12.62	13.00	12.93	−12.97
2	0.57	−0.58	−0.58	0.58
3	3.81	−3.83	−3.86	3.90
4	3.26	−3.36	−3.33	3.34
5	−2.26	2.37	2.32	−2.34
6[b]	4.37	−3.59	−3.48	3.51
7[b]	−0.52	0.53	0.49	−0.51

[a] Methyl group is in quadrant I. (See Table VI.) Type 3 couplings are unimportant for compounds 1 and 3. [b] Type 6 coupling: (C_β, β_{eq}), (S, S). Type 7 coupling: (C_β, β_{ax}), (S, S).

the discussion given above about the detailed atom and bond coupling terms can be carried over to the ketones with no qualitative change. Thus, the same mechanism for n–π* optical activity appear to operate in both the ketones and the thioketones, and the revised octant rule[19] appears to hold in the latter class as well.

Concluding Remarks

We have shown, experimentally and theoretically, that the chiroptical properties of the long-wavelength band in a number of thioketones and their keto analogues are remarkably similar. Calculations in the random-phase approximation yielded n–π* rotatory strengths in very good agreement with the observed ones for methyl adamantanones as well as their thio analogues. The present ab initio RPA calculations and our previous ones on a diethyl ketone model system[34] support the qualitative results and analysis in our earlier CNDO/S study of the ketone octant rule.[19] The dominant coupling types that we extract here and the one- and two-center analysis of the electric dipole transition moment in ref 19 can be attributed to the large magnetic moment and predominance of the n–π* *configuration* in the overall excitation description. The ab initio MOs and RPA in this case provide the needed correction terms to bring the magnitude of the rotatory strengths into line with experiment. Near the nodal surfaces predicted by our earlier CNDO/S work, the RPA appears to be necessary to account satisfactorily for observed sensitivities. The methods of analyzing the computed intensities discussed here allowed extraction of structural couplings responsible for the optical activity. The CD spectra, in conjunction with the UV spectra, constituted both a sensitive structural probe and a useful adjunct in studying the nature of the electronic excitations.

Experimental Section

General. Circular dichroism (CD) spectra were recorded on a JASCO J-40 instrument equipped with a photoelastic modulator and a J-DPY data processor. Ultraviolet spectra were recorded on a Cary 219 spectrophotometer, and rotations were determined in 96% ethanol unless otherwise indicated on a Perkin-Elmer 141 polarimeter. All nuclear magnetic resonance (NMR) spectra were determined in $CDCl_3$ and reported in δ (ppm) downfield from tetramethylsilane unless otherwise indicated on a Perkin-Elmer R-24B or JEOL FX-100 instrument. Mass spectra (MS) were recorded at 70-eV ionizing voltage on a Kratos MS-50 mass spectrometer at the Midwest Center for Mass Spectrometry, University of Nebraska, Lincoln. Infrared (IR) spectra were measured on a Perkin-Elmer Model 599 instrument. All melting points are uncorrected and were determined on a Thomas-Hoover or Mel-Temp capillary apparatus. Analytical gas chromatography (GC) was performed on a Varian-Aerograph model 2400 F/I instrument using a 6 ft × $^3/_8$ in. diameter column (A) with 5% FFAP stationary phase adsorbed on 80/100 Chromosorb W AW-DMCS. Preparative gas chromatography (GC) was performed on a 5 ft × $^3/_8$ in. diameter column (B) (15% QF-1 on 80/100 Chromosorb W) with a Varian-Aerograph Model 1720 T/C instrument.

Spectral data were obtained with spectra grade solvents (MCB): *n*-heptane, isooctane, *p*-dioxane, MI 4:1 (methylcyclohexane–isopentane; 4:1, v/v), perfluoropentane (3 M), and EPA (ethyl ether–isopentane–ethanol; 5:5:2, v/v/v). Diethyl ether was first distilled from CaH_2 and then from $LiAlH_4$ all under N_2. Other solvents used were freshly distilled or stored over 4-Å molecular sieves (Linde). Phosphorus pentasulfide was from Baker and lithium aluminum deuteride (99%) was from Stohler.

(+)-(1*S*,3*R*,5*R*)-*endo*-(3-Bicyclo[3.3.1]non-6-enyl) Methyl Ketone (8).[40] One gram (6.02 mmol) of (+)-(3*R*)-*endo*-3-Bicyclo[3.3.1]non-6-enecarboxylic acid (7) ($[\alpha]^{25}_{578}$ +79.6° (*c* 1.0), 52.97% ee[22]) was dissolved in dry ethyl ether and converted to its lithium salt by the addition of 50 mg of finely powdered LiH. The mixture was stirred at room temperature for 1 h; then the solvent was removed by rotary evaporation. The resulting lithium salt was dried under vacuum at 80 °C. The dried salt (1.00 g) in 25 mL of dry ether was stirred vigorously while an ethereal solution of methyllithium (1.52 M, 5 mL, 7.6 mmol) was added to it at 0 °C. The mixture was stirred for 0.5 h at 0 °C after final addition and then 3 h at room temperature, after which it was quenched by the addition of saturated aqueous NH_4Cl. The aqueous layer was separated and extracted with (3 × 25 mL) ether. The combined ether layers were washed with water (25 mL) then with 5% aqueous $NaHCO_3$ and dried ($MgSO_4$). Evaporation of the ether gave a pale yellow oil which was distilled (Kugelrohr, 78 °C, 2 mm) [lit.[40] bp 70–73 °C (0.5 mm)] to give 0.86 g (87%) of the colorless, semisolid ketone **8**: 99% pure by GC on column A; $[\alpha]^{25}_{589}$ +63.01°, $[\alpha]^{35}_{578}$ +64.97° (*c* 1.1); IR (neat) 3040, 1719, 1350 cm^{-1}; ^1H NMR δ 1.2–2.7 (br m, 11 H), 2.0 (s, 3 H, CH_3), 5.2–5.7 (m, 2 H, =CH).

(+)-(2*S*,5*R*,3*R*)-*endo*-3-(1-Hydroxyethyl)bicyclo[3.3.1]non-6-ene (9). Ketone **8** from above (0.75 g, 4.6 mmol) in 20 mL of dry ether was added dropwise to stirred slurry of $LiAlH_4$ (0.24 g) in ether (20 mL). The mixture was heated to reflux following complete addition. After 4 h at reflux, the mixture was cooled and added to 50 mL of a 1:1 mixture of water–10% aqueous H_2SO_4. The aqueous layer was separated and extracted with ether (3 × 25 mL). The combined ether layers were washed with water (25 mL) and then 5% aqueous $NaHCO_3$ and dried ($MgSO_4$). After removal of the solvent by rotary evaporation and Kugelrohr (94 °C, 2.5 mm) distillation, 0.68 g (90%) of alcohol **9** was obtained: 99% pure by GC on column A; $[\alpha]^{25}_{589}$ +115.7°, $[\alpha]^{35}_{578}$ +121.8° (*c* 0.99); IR (neat) 3600–3200, 3025 cm^{-1}; ^1H NMR, δ 0.9–2.5 (br, m, 11 H), 1.0 (d, 3 H, *J* = 6 Hz, CH_3), 3.4 (br 1 H, OH), 5.51–5.9 (br t, 2 H, =CH).

Anal. Calcd for $C_{11}H_{18}O$ (166): C, 79.46; H, 10.91. Found: C, 79.20; H, 10.77.

(+)-(1*S*,3*R*,4*S*)-4(a)-Methyladamantan-2-one (2).[23a,24b] Alcohol **9** (0.60 g, 3.6 mmol) from above was heated in formic acid (88%, 10 mL) at 100 °C. After heating 4 h, the solution was cooled, poured into water (25 mL), and basified with 50% aqueous NaOH. The products were extracted with ether (3 × 25 mL), and the combined ether extracts were washed with water (2 × 25 mL) and dried ($MgSO_4$). Evaporation of the ether gave a mixture of pale yellow liquid formate esters. Hydrolysis was achieved by dissolving the esters in ether (20 mL) and adding the ether solution dropwise to a stirred slurry of $LiAlH_4$ in ether (20 mL). The mixture was heated at reflux for 1 h after complete addition, cooled, and quenched by adding to 50 mL of a 1:1 mixture of water–10% aqueous H_2SO_4. The desired alcohol mixture (**9**) was obtained by using ether extraction, and the alcohol mixture in acetone was oxidized to the corresponding ketones (**1** and **3**) by Jones reagent.[41] Excess oxidant was decomposed by adding 2-propanol. The solution was diluted with ether (25 mL) and neutralized with 5% aqueous $NaHCO_3$. Solids were removed by filtration, the filtrate extracted with ether, and the ether layer dried ($MgSO_4$) to give a pale yellow solid. The solid was sublimed (110 °C, 1 atm) to yield white crystals (470 mg, 80%) of a 1:1 mixture of **1**

and **3** (GC, column A). The mixture was separated by preparative GC on column B to give a 40% yield of 99% pure **1**: mp 187–189 °C (sealed capillary) (lit.[24b] mp 185–187 °C); $[\alpha]^{25}_{589}$ +10.11°, $[\alpha]^{25}_{578}$ +10.62, $[\alpha]^{25}_{436}$ +20.29, $[\alpha]^{25}_{365}$ +30.15 (*c* 0.68); UV (MI 4:1) $\Delta\epsilon_{290}^{max}$ 17; UV (EPA) ϵ_{287}^{max} 21; CD (MI 4:1) $\Delta\epsilon_{250}$ 0, $\Delta\epsilon_{281.5}$ +0.020, $\Delta\epsilon_{291}$ +0.022, $\Delta\epsilon_{301}$ +0.023, $\Delta\epsilon_{312.5}$ +0.025, $\Delta\epsilon_{323.5}$ +0.013, $\Delta\epsilon_{339}$ 0; CD (EPA) $\Delta\epsilon_{272}$ 0, $\Delta\epsilon_{288}$ −0.026, $\Delta\epsilon_{296.5}$ −0.045, $\Delta\epsilon_{305.5}$ −0.046, $\Delta\epsilon_{316}$ −0.019, $\Delta\epsilon_{321}$ 0 (CD run at room temperature and data corrected to 100% ee); IR (CCl_4) 2920, 2860, 1715, 1065 cm^{-1}; ^1H NMR δ 0.95 (d, 3 H, J = 7 Hz, CH_3), 1.6–2.55 (br m, 13 H); ^{13}C NMR in Table I; MS, m/z (relative intensity) 164.1199 (M^+; calcd for $C_{11}H_{16}O$, 164.1201) (100%), 95 (28%), 94 (51%), 93 (40%), 80 (27%), 79 (49%).

(+)-(1*S*,3*R*,4*R*)-4(e)-Methyladamantan-2-one (4).[23b,c,24b] The equatorial methyl epimer (**4**) formed and separated above by preparative GC had mp 165–167 °C (sealed capillary); $[\alpha]^{25}_{D} \simeq 0°$, $[\alpha]^{25}_{578} \simeq 0°$, $[\alpha]^{25}_{436}$ +11.19°, $[\alpha]^{25}_{365}$ +54.29° (*c* 0.97); UV (MI 4:1) ϵ_{293}^{max} 19; UV (EPA) ϵ_{290}^{max} 22; CD (MI 4:1) $\Delta\epsilon_{252}$ 0, $\Delta\epsilon_{287}$ +0.393, $\Delta\epsilon_{295.5}$ +0.479, $\Delta\epsilon_{305}$ +0.544, $\Delta\epsilon_{316.5}$ +0.362, $\Delta\epsilon_{332}$ 0; CD (EPA) $\Delta\epsilon_{242}$ 0, $\Delta\epsilon_{294.5}$ +0.671, $\Delta\epsilon_{303}$ +0.643, $\Delta\epsilon_{310}$ +0.306, $\Delta\epsilon_{332}$ 0 (CD run at room temperature and values corrected to 100% ee); IR ($CHCl_3$) 2920, 2860, 1710, 1055 cm^{-1}; ^1H NMR δ 1.07 (d, 3 H, J = 7 Hz, CH_3), 1.4–2.47 (br m, 13 H); ^{13}C NMR in Table I; MS, m/z (relative intensity) 164.1191 (M^+; calcd for $C_{11}H_{16}O$, 164.1201) (100%), 95 (31%), 94 (75%), 93 (84%), 81 (25%), 79 (59%).

(+)-(1*S*,3*R*,4*S*)-4(a)-Methyladamantan-2-thione (1). An epimeric mixture of 4(a)-methyladamantan-2-one (**2**) and 4(e)-methyladamantan-2-one (**4**) (110 mg, 0.67 mmol, enantiomeric excess 52.97%) was added to a solution of phosphorus pentasulfide (40 mg, 0.09 mmol) in dry pyridine (1 mL). The mixture was heated at slow reflux while keeping it well stirred. The air inside the reaction flask was flushed out with dry nitrogen. After a period of 16 h, the mixture was added to petroleum ether (15 mL, 40–60 °C). The mixture was extracted first with water (4 × 5 mL), then with 2 N HCl (2 × 5 mL), and finally with water (2 × 5 mL). The aqueous layers were discarded and the organic layer was dried overnight with anhydrous $MgSO_4$. Removal of the solvent under reduced pressure yielded an orange mass. This crude mixture was chromatographed on silica gel by using a petroleum ether (40–60 °C)/benzene mixture (88/12) to obtain a purified mixture of epimeric thioketones. The yield at this point was 84 mg (70%). The final separation of the two epimers was achieved by preparative gas chromatography to afford 99% pure thioketones **1** and **3**. The red-orange, crystalline axial methyl thioketone **1** had mp 162–163 °C; $[\alpha]^{25}_{589}$ +11.0°, $[\alpha]^{25}_{578}$ +16.49° (*c* 0.07, *n*-heptane); UV (MI 4:1) ϵ_{517} 11.4, ϵ_{505} 11.3, ϵ_{491} 11.4; UV (*n*-heptane) ϵ_{242} 12,500; UV (*p*-dioxane) ϵ_{505} 11.3, ϵ_{484} 11.9; CD (MI 4:1) $\Delta\epsilon_{544}$ 0, $\Delta\epsilon_{514}$ −0.029, $\Delta\epsilon_{494}$ −0.004, $\Delta\epsilon_{484}$ −0.003, $\Delta\epsilon_{479}$ 0, $\Delta\epsilon_{243}$ −4.3, $\Delta\epsilon_{238}$ 0.0, $\Delta\epsilon_{217}$ +10.4; CD (*p*-dioxane) $\Delta\epsilon_{544}$ 0, $\Delta\epsilon_{505}$ −0.117, $\Delta\epsilon_{485}$ −0.078, $\Delta\epsilon_{420}$ 0 (CD run at room temperature and data corrected to 100% ee); IR (CH_2Cl_2) 2930, 1450, 1390, 1305, 1150 (C=S) cm^{-1}; ^1H NMR (CD_2Cl_2) δ 0.94 (d, 3 H, J = 7.1 Hz), 1.6–2.47 (br m, 11 H), 3.23 (br s, 1 H), 3.33 (br s, 1 H); ^{13}C NMR in Table I; MS, m/z (relative intensity) 180.0972 (M^+; calcd for $C_{11}H_{16}S$, 180.09726) (100%), 175 (5%), 147 (35%), 139 (16%).

Anal. Calcd for $C_{11}H_{16}S$ (180): C, 73.27%; H, 8.94%; S, 17.78%. Found: C, 73.22%; H, 8.84%; S, 17.80%.

(+)-(1*S*,3*R*,4*R*)-4(e)-Methyladamantane-2-thione (3). The crystalline red-orange equatorial methyl epimer (**3**), found and separated above by preparative GC, had mp 81–82 °C; $[\alpha]^{25}_{589}$ +47.14°, $[\alpha]^{25}_{578}$ +58.13°, $[\alpha]^{25}_{436}$ −340.95°, $[\alpha]^{25}_{365}$ −326.81° (*c* 0.12, *n*-heptane); UV (MI 4:1) ϵ_{513} 12.5, ϵ_{505} 12.6, ϵ_{490} 12.5; UV (*n*-heptane) ϵ_{241} 11,900; UV (*p*-dioxane) ϵ_{498} 12.7, ϵ_{484} 12.7; CD (MI 4:1) $\Delta\epsilon_{553}$ 0, $\Delta\epsilon_{515}$ +0.563, $\Delta\epsilon_{420}$ 0; CD (*n*-heptane) $\Delta\epsilon_{267}$ 0, $\Delta\epsilon_{240}$ −5.07, $\Delta\epsilon_{219}$ −2.67, $\Delta\epsilon_{212}$ 0 (CD run at room temperature and values corrected to 100% ee); IR (nujol) 1450, 1375, 1150 (C=S) cm^{-1}; ^1H NMR ($CDCl_3$) δ 1.14 (d, 3 H, J = 7.1 Hz), 1.31–2.33 (br m, 11 H), 3.11 (br s, 1 H), 3.35 (br s, 1 H); ^{13}C NMR in Table I; MS, m/z (relative intensity) 180.0971 (M^+; calcd for $C_{11}H_{16}S$, 180.09726) (100%), 165 (5%), 147 (36%), 139 (16%).

Anal. Calcd for $C_{11}H_{16}S$ (180): C, 73.27%, H, 8.94%, S, 17.78%. Found: C, 73.43%; H, 8.68%; S, 17.80%.

(+)-(1*S*,5*R*,3*R*)-*endo*-3-(Hydroxydideuteriomethyl)bicyclo[3.3.1]non-6-ene (10).[17] (+)-*endo*-Bicyclo[3.3.1]non-6-ene-3*R*-carboxylic acid (**7**) (900 mg, 5.42 mmol) ($[\alpha]^{25}_{578}$ +49.32° (*c* 1.1), 32.82% ee[22]) was converted to its methyl ester using diazomethane according to the procedure described by McKervey et al.[42] The methyl ester (760 mg, 4.22 mmol) dissolved in dry ether (10 mL) was added dropwise to a stirred slurry of $LiAlD_4$ (710 mg, 16.9 mmol) in ether (5 mL). After the addition was complete the mixture was heated at reflux for a period of 3 h, after which it was quenched with water. The aqueous layer was separated and extracted with ether (3 × 20 mL). The combined ether layers were washed with watter (3 × 20 mL) and dried over anhydrous $MgSO_4$. Evaporation of ether under reduced pressure gave a pale yellow liquid. Reduced pressure distillation (Kugelrohr) of the yellow liquid yielded 600 mg (72%) of a colorless oil: bp 123–126 °C (1.8 mm); $[\alpha]^{25}_{589}$ +70.58°, $[\alpha]^{25}_{578}$ +73.95° (*c* 1.0); IR (neat) 3330, 2900, 2180, 2640, 965 cm^{-1}; ^1H NMR ($CDCl_3$) δ 1.80 (br m, 11 H), 3.68 (br 1 H, OH), 5.62 (br m, 2 H, HC=CH).

(−)-(1*S*,3*R*)-4,4-Dideuterioadamantan-2-one (6).[17b] 3-(Hydroxydideuteriomethyl)bicyclo[3.3.1]non-6-ene (500 mg, 3.25 mmol) ($[\alpha]^{25}_{578}$ +73.94° (*c* 1.0), 32.82% ee) was dissolved in aqueous formic acid (88%, 10 mL). The solution was heated at 100 °C for a period of 3 h. Then it was cooled, poured into water (10 mL), and basified with 50% aqueous NaOH. The organic substances were extracted with ether (4 × 20 mL). The combined ether layers, after washing with water (20 mL), were dried over anhydrous $MgSO_4$. Evaporation of ether under reduced pressure gave a pale yellow solid. This solid, which consisted of a mixture of formate esters (by GC), was hydrolyzed to the corresponding alcohols as follows. The above solid dissolved in dry ether (5 mL) was added slowly to a stirred slurry of $LiAlH_4$ (500 mg) in ether (10 mL). After the addition was complete, the mixture was heated at reflux for a period of 0.5 h and then quenched by adding to water (20 mL). The ether layer was separated, the aqueous layer was extracted with ether (3 × 20 mL), and all ethereal layers were combined. The combined ether layers were first washed with dilute HCl (10%, 25 mL), then with water (25 mL), and finally with aqueous $NaHCO_3$ (5%, 25 mL). After drying with anhydrous $MgSO_4$, the ether was removed under reduced pressure to obtain a white solid, which consisted of epimeric cyclic alcohols (**12**). The yield of crude product was 444 mg. The above crude product was oxidized to a white, solid ketone with Jones' reagent.[41] Sublimation of the ketone (150 °C) yielded 357 mg (72%) of product **6**: mp 254–256 °C; $[\alpha]^{25}_{589}$ −1.11, $[\alpha]^{25}_{576}$ −1.35, $[\alpha]^{25}_{546}$ −1.59, $[\alpha]^{25}_{436}$ −3.33, $[\alpha]^{25}_{365}$ −8.73 (*c* 0.63, isooctane); UV (isooctane) ϵ_{293}^{max} 18.1; CD (isooctane) $\Delta\epsilon_{330}$ 0, $\Delta\epsilon_{316}$ −0.058, $\Delta\epsilon_{305}$ −0.099, $\Delta\epsilon_{295}$ −0.103, $\Delta\epsilon_{280}$ −0.076, $\Delta\epsilon_{250}$ 0 (CD run at room temperature and values corrected to 100% ee); IR (nujol) 2200, 2100, 1730 cm^{-1}; ^1H NMR ($CDCl_3$) δ 1.86 (s, 2 H), 1.96 (br s, 8 H), 2.46 (br s, 2 H); ^{13}C NMR in Table I; MS, m/z (relative intensity) 152.1169 (M^+; calcd for $C_{10}H_{12}D_2O$, 152.1170) (100%), 119 ($C_9H_7D_2$) (10%), 95 ($C_7H_7D_2$) (11%), 83.0826 ($C_6H_7D_2$) (29%), 80.0614 (C_6H_6O) (69%).

(−)-(1*S*,3*R*)-4,4-Dideuterioadamantan-2-thione (5).[17a] Phosphorus pentasulfide (29.3 mg, 0.066 mmol) was added in one portion to a solution of 4,4-dideuterioadamantan-2-one (**6**, prepared above) (80 mg, 0.53 mmol, 32.82% ee) in dry pyridine (2 mL). The solution was heated at 90 °C for a period of 11 h. Then it was cooled and added to petroleum ether (40–60 °C, 20 mL). The yellow residue left behind in the reaction flask was also washed with petroleum ether (2 × 5 mL) and added to the previous solution. The combined solution was washed with water (2 × 10 mL) followed by 2 N HCl (2 × 10 mL) and finally with cold water (2 × 10 mL). The aqueous solutions were discarded, and the orange organic layer, after drying with anhydrous $MgSO_4$, was evaporated under reduced pressure to yield and orange solid. GC analysis showed the presence of a slight amount of unreacted ketone. The thione was successfully purified by sublimation at atmospheric pressure and 90–100 °C (77 mg, 87%) to give red-orange crystals of thione **5**: mp 167–170° (lit.[3] mp for the protio thione 173–174 °C); $[\alpha]^{21}_{589}$ −5.68°, $[\alpha]^{21}_{578}$ −7.3°, $[\alpha]^{21}_{365}$ +12.16°, $[\alpha]^{21}_{436}$ +3.24° (*c* 0.25, isooctane); UV (isooctane) ϵ_{514} 11.5, ϵ_{502} 11.7, ϵ_{480} 11.7, ϵ_{239} 12900; CD (isooctane) $\Delta\epsilon_{550}$ 0.0, $\Delta\epsilon_{519}$ −0.039, $\Delta\epsilon_{508}$ −0.041, $\Delta\epsilon_{495}$ −0.039, $\Delta\epsilon_{485}$ −0.032, $\Delta\epsilon_{425}$ 0; CD (*n*-heptane) $\Delta\epsilon_{550}$ 0.0, $\Delta\epsilon_{518}$ −0.040, $\Delta\epsilon_{507}$ −0.041, $\Delta\epsilon_{494}$ −0.04, $\Delta\epsilon_{485}$ −0.032, $\Delta\epsilon_{428}$ 0.0, $\Delta\epsilon_{252}$ −0.23, $\Delta\epsilon_{238}$ 0.0, $\Delta\epsilon_{220}$ +0.53 (CD run at room temperature and values corrected to 100% ee); IR (nujol) 2200, 2080, 1450, 1375, 1150 (C=S) cm^{-1}; ^1H NMR ($CDCl_3$) δ 1.99 (br s, 4 H), 2.07 (br s, 6 H), 3.39 (br s, 2 H); ^{13}C NMR in Table I; MS, m/z (relative intensity) 168.0940 (M^+; calcd for $C_{10}H_{12}D_2S$, 168.094 17) (100%), 135 (19%).

Computational Details. Hartree–Fock–Roothaan self-consistent MOs were obtained for all molecules from the GAUSSIAN 76 program system,[43a] locally modified to handle basis sets up to 127 atomic orbitals and to interface with program RPAC;[44] the latter program was used for the excitation calculations. The minimal basis set (A) was the standard STO-4G set,[43b] and the split-valence basis (B) was the built-in 4/31G (44/31G on S) basis.[43c] The extended basis (C) was obtained from basis B by the addition of a double set of d-type Gaussian functions (α_d = 0.55, 0.015) to the sulfur atom, and a single set of diffuse s and p Gaussian functions to the atoms of the C=S group (C, α_s = 0.023, α_p = 0.021; S, α_s = 0.023, α_p = 0.020). Geometrical parameters for the thioacetone and methyl ethyl thioketone were taken from Dreiding models: r(C=S) = 1.68 Å, r(C—C) = 1.47 Å, r(C—C) = 1.54 Å, r(C—H) = 1.09 Å. Angles: C—C=S, 122°; C—C—C, 109.5°; H—C—H, 109.5°; C—C—C=S, 120°. For the adamantane derivatives **1–4**, an idealized adamantane skeleton was used, with all r(C—C) = 1.54 Å, r(C—H) = 1.09 Å, r(C=S) = 1.68 Å, r(C=O) = 1.22 Å, and all CCC and HCH angles tetrahedral. The C—C=X (X = S, O) angle was 125.3°, and the methyl

group was staggered, except for **1-3**, where both staggered and eclipsed forms were used.

Basis sets A, B, and C yielded total RHF energies of respectively (thioacetone) (N = 30) -512.709 103, (N = 52) -513.966 854, (N = 70) -514.000 128 au (1 au = 627.5 kcal/mol); (methyl ethyl thioketone) (N = 37) -551.637 418, (N = 65) -552.940 938, (N = 83) -552.974 289 au. Basis A yielded the following RHF energies (all in au) for 1-4: (**1**, staggered, N = 80) -819.322 491; (**1**, eclipsed, N = 80) -819.317 254, (**2**, staggered, N = 76) -498.294 136, (**2**, eclipsed, N = 76) -498.288 907, (**3**, staggered, N = 80) -829.319 224, (**3**, eclipsed, N = 80) -819.314 474, (**4**, staggered, N = 76) -498.290 552.

The RPA calculations included all possible single excitations, excluding those out of the core MOs, supported by the MO basis. For thioacetone, bases A, B, and C yielded 120, 384, and 600 configurations, respectively, while for methyl ethyl thioketone there were 195, 615, and 885 configurations. For **1-4**, the RPA calculations included 1023 configurations for each molecule.

Acknowledgment. We thank the NATO Scientific Affairs Division for a grant (RG.138.81) in support of this work. Aa.E.H thanks the Danish Natural Science Research Council for travel support (Grant 11-3574/1982). D.A.L. and T.D.B. thank the National Science Foundation (CHE 8218216) and the donors of the Petroleum Research Fund, administered by the American Chemical Society, for support of this work. Generous grants of computer time were provided by Southern Illinois University at Edwardsville (T.D.B) and the University of Copenhagen (T.D.B., Aa.E.H). We thank also Drs. K. Schaumburg, J. Sandström, and R. E. Viola for helpful discussions.

Electrostatic Effects in Interactions between Hard (Soft) Acids and Bases†

Roman F. Nalewajski‡

Contribution from the Institute for Theoretical Chemistry and the Department of Chemistry, University of Texas, Austin, Texas 78712. *Received June 10, 1983*

Abstract: Recent theoretical deduction of the principle of hard and soft Lewis acids and bases (HSAB) by Parr and Pearson is commented upon and extended to explicitly include the electrostatic effects accompanying the formation of a chemical bond. The present explanation of the HSAB principle is based on a modified energy expression for an atom-in-a-molecule, suggested by the density functional theory, and the chemical potential (electronegativity) equalization principle.

This article comments upon and extends the recent remarkable theoretical deduction by Parr and Pearson[1] of the Principle of Hard and Soft Acids and Bases (HSAB).[2]

According to this principle hard Lewis acids prefer to coordinate to hard Lewis bases, and soft acids to soft bases, with the soft–soft interactions being largely covalent and the hard–hard interactions predominantly ionic. In an attempt to quantify and theoretically justify the HSAB principle Parr and Pearson have introduced the concept of *absolute hardness*:

$$\eta = \tfrac{1}{2}(\partial^2 E/\partial N^2)_Z = \tfrac{1}{2}(\partial\mu/\partial N)_Z = -\tfrac{1}{2}(\partial\chi/\partial N)_N = \tfrac{1}{2}(I - A) \quad (1)$$

where $E = E(N,Z)$ is the energy, N is the number of electrons, Z is the atomic number of the donor (or acceptor) atom, $\mu = (\partial E/\partial N)_Z$ is the chemical potential, and $\chi = -\mu = {}^1/_2(I + A)$ is the electronegativity; here I and A are the ionization potential and electron affinity of the species in question. The absolute hardness, positive by the stability criterion,[3] is large for hard species and small for soft ones. It is one of the three *stiffness moduli* defining the *stiffness matrix* of the second derivatives of $E(N,Z)$.[4] With use of the energy expression (superscript degree refers to the isolated reactants)

$$E(N) = E^\circ + \mu^\circ(N - N^\circ) + \eta(N - N^\circ)^2 = E^\circ + \mu^\circ\Delta N + \eta(\Delta N)^2 \quad (2)$$

for an atom-in-a-molecule, and the chemical potential (electronegativity) equilization principle[5] (to determine ΔN) gives the stabilization energy for the A–B complex:[1]

$$\Delta E = (E_A - E_A^\circ) + (E_B - E_B^\circ) = [(\mu_A^\circ - \mu_B^\circ)\Delta N] + [(\eta_A + \eta_B)(\Delta N)^2] = \left[-\tfrac{1}{2}\frac{(\mu_B^\circ - \mu_A^\circ)}{\eta_A + \eta_B}\right] + \left[\tfrac{1}{4}\frac{(\mu_B^\circ - \mu_A^\circ)^2}{\eta_A + \eta_B}\right] = -\tfrac{1}{4}\frac{(\mu_B^\circ - \mu_A^\circ)^2}{\eta_A + \eta_B} \quad (3)$$

here ΔN is the electron transfer from B (donor atom of a base) to A (acceptor atom of an acid). This expression immediately explains the soft–soft preference of the HSAB principle, since then both η_A and η_B are small and stabilization of the complex large. It does not explain, however, the hard–hard preference (large denominator). To resolve this apparent paradox Parr and Pearson attributed stability of the hard–hard interaction to the ionic bond which should be favorable in this case. Equation 3, supplemented by an extra-stabilization expected from the equalization of ionization potentials of atoms-in-a-molecule, offers a "proof" of the HSAB principle.[1]

A major defect of this deduction, and—as we shall demonstrate—the reason for the hard–hard paradox, is that, while including second-order effects due to electron transfer in energy expressions 2 and 3, it neglects important *first-order contributions*

†Supported in part by a research grant from the National Science Foundation and a grant from the Institute of Low Temperatures and Structural Research, Polish Academy of Sciences, Wrocław, Poland.

‡On leave from the Department of Theoretical Chemistry, Jagiellonian University, Cracow, Poland.

(1) R. G. Parr and R. G. Pearson, *J. Am. Chem. Soc.*, in press.
(2) R. G. Pearson, "Hard and Soft Acids and Bases", Dowden, Hutchinson and Ross, Stroudenburg, PA, 1973; T. L. Ho, "Hard and Soft Acids and Bases in Organic Chemistry", Academic Press, New York, 1977; W. B. Jensen, "The Lewis Acid–Base Concept", Wiley-Interscience, New York, 1980, Chapter 8.
(3) R. F. Nalewajski and J. F. Capitani, *J. Chem. Phys.*, **77**, 2514–26 (1982); R. F. Nalewajski, *ibid.*, in press.
(4) H. B. Callen, "Thermodynamics", Wiley, New York, 1960, Appendix G.
(5) H. K. Ray, L. Samuels, and R. G. Parr, *J. Chem. Phys.*, **70**, 3680–84 (1979); R. G. Parr and L. J. Bartolotti, *J. Am. Chem. Soc.*, **104**, 3801–3 (1982).

0002-7863/84/1506-0944$01.50/0